

## Neutron-rich $\Lambda$ -Hypernuclei study with the FINUDA experiment

E. Botta<sup>1,2,a</sup>

<sup>1</sup>INFN Sezione di Torino, via P. Giuria 1, Torino, Italy

<sup>2</sup>Dipartimento di Fisica, Università di Torino, via P. Giuria 1, Torino, Italy

**Abstract.** The FINUDA experiment at DAΦNE, Frascati, has found evidence for the neutron-rich hypernucleus  ${}^6_{\Lambda}\text{H}$  studying  $(\pi^+, \pi^-)$  pairs in coincidence from the  $K_{\text{stop}}^- + {}^6\text{Li} \rightarrow {}^6_{\Lambda}\text{H} + \pi^+$  production reaction followed by  ${}^6_{\Lambda}\text{H} \rightarrow {}^6\text{He} + \pi^-$  weak decay. The production rate of  ${}^6_{\Lambda}\text{H}$  undergoing this two-body  $\pi^-$  decay has been found to be  $(2.9 \pm 2.0) \cdot 10^{-6}/K_{\text{stop}}^-$ . Its binding energy has been evaluated to be  $B_{\Lambda}({}^6_{\Lambda}\text{H}) = (4.0 \pm 1.1)$  MeV with respect to  $({}^3\text{H} + \Lambda)$ , jointly from production and decay. A systematic difference of  $(0.98 \pm 0.74)$  MeV between  $B_{\Lambda}$  values derived separately from decay and from production has been tentatively assigned to the  ${}^6_{\Lambda}\text{H } 0_{\text{g.s.}}^+ \rightarrow 1^+$  excitation.

A similar investigation has been carried out for the neutron-rich hypernucleus  ${}^9_{\Lambda}\text{He}$  studying the  $K_{\text{stop}}^- + {}^9\text{Be} \rightarrow {}^9_{\Lambda}\text{He} + \pi^+$  reaction in coincidence with the  ${}^9_{\Lambda}\text{He} \rightarrow {}^9\text{Li} + \pi^-$  weak decay; an upper limit for the production rate of  ${}^9_{\Lambda}\text{He}$  undergoing the two-body  $\pi^-$  decay has been found to be  $4.2 \cdot 10^{-6}/K_{\text{stop}}^-$  (90% C.L.).

### 1 Introduction

The role of the  $\Lambda$  hyperon in stabilizing nuclear cores was pointed out in the early '60 by Dalitz and Levi Setti [1] discussing the existence of light hypernuclei with large neutron excess. This feature is demonstrated by the observation of  ${}^6_{\Lambda}\text{He}$ ,  ${}^7_{\Lambda}\text{Be}$ ,  ${}^8_{\Lambda}\text{He}$ ,  ${}^9_{\Lambda}\text{Be}$  and  ${}^{10}_{\Lambda}\text{B}$  hypernuclei in emulsion experiments [2]. No unstable-core hydrogen  $\Lambda$  hypernuclei have been found so far, although the existence of the lightest possible one  ${}^6_{\Lambda}\text{H}$  was predicted in [1] and subsequently reinforced in estimates by Majling [3]. The neutral-baryon excess in  ${}^6_{\Lambda}\text{H}$ , in particular, would be  $(N + Y)/Z = 5$ , with  $Y = 1$  for a  $\Lambda$  hyperon, or  $N/Z = 4$ , larger than the maximal value in light nuclei,  $N/Z = 3$  for  ${}^8\text{He}$  [4]. Neutron-rich light hypernuclei could thus go beyond the neutron drip line for ordinary nuclear systems. The study of  ${}^6_{\Lambda}\text{H}$  and of heavier neutron-rich hypernuclei could place valuable constraints on the size of coherent  $\Lambda N - \Sigma N$  mixing in dense strange neutron-rich matter [5] with immediate impact on the stiffness/softness of the equation of state for hyperons in neutron-star matter [6].

Neutron rich hypernuclei could be produced by the two-body double charge-exchange reactions:

$$K^- + {}^AZ \rightarrow {}^A_{\Lambda}(Z - 2) + \pi^+, \quad (1)$$

induced on nuclear targets by stopped or in flight  $K^-$  mesons, and

$$\pi^- + {}^AZ \rightarrow {}^A_{\Lambda}(Z - 2) + K^+ \quad (2)$$

<sup>a</sup>e-mail: botta@to.infn.it

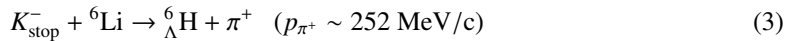
with  $\pi^-$  mesons in flight ( $p_{\pi^-} > 0.89$  GeV/c).

These reactions can be described as two-step processes on two different protons of the same nucleus, which convert them first into a neutron and then into a  $\Lambda$ , with the additional condition that the final nuclear system is bound. Another mechanism could be a single-step double charge exchange  $m_i^- p \rightarrow \Sigma^- m_f^+$  (where  $m$  stands for meson) feeding the  $\Sigma$  component coherently admixed into the final  $\Lambda$  hypernuclear state. The two-step processes are expected to occur at a rate  $\leq 10^{-2}$  smaller [7] than the production of normal  $\Lambda$  hypernuclei by means of the corresponding single-step 2-body reactions ( $K^-, \pi^-$ ) and ( $\pi^+, K^+$ ).

The first experimental attempt to produce neutron-rich hypernuclei was carried out at KEK [8] by the reaction (1) with  $K^-$  at rest. Upper limits were obtained for the production of  ${}^9_{\Lambda}\text{He}$ ,  ${}^{12}_{\Lambda}\text{Be}$  and  ${}^{16}_{\Lambda}\text{C}$  hypernuclei (on  ${}^9\text{Be}$ ,  ${}^{12}\text{C}$  and  ${}^{16}\text{O}$  targets respectively) in the range of  $(0.6 - 2.0) \cdot 10^{-4}/K_{\text{stop}}^-$ . Another KEK experiment [9] reported the production of  ${}^{10}_{\Lambda}\text{Li}$  in the  $(\pi^-, K^+)$  reaction on a  ${}^{10}\text{B}$  target using a 1.2 GeV/c  $\pi^-$  beam, with a cross section of  $(11.3 \pm 1.9)$  nb/sr in the  $\Lambda$ -bound region.

A further attempt to observe neutron-rich hypernuclei by means of the reaction (1) with  $K^-$  at rest, was made at the DAΦNE collider at LNF by the FINUDA experiment [10], on  ${}^6\text{Li}$  and  ${}^7\text{Li}$  targets. From the analysis of a partial data sample, upper limits were evaluated for  $\Lambda$  hypernuclear production:  $R_{\pi^+}({}^6_{\Lambda}\text{H}) < (2.5 \pm 0.4_{\text{stat}}^{+0.4}_{-0.1\text{syst}}) \cdot 10^{-5}/K_{\text{stop}}^-$ ,  $R_{\pi^+}({}^7_{\Lambda}\text{H}) < (4.5 \pm 0.9_{\text{stat}}^{+0.4}_{-0.1\text{syst}}) \cdot 10^{-5}/K_{\text{stop}}^-$ . In addition an upper limit was estimated for  ${}^{12}_{\Lambda}\text{Be}$ :  $R_{\pi^+}({}^{12}_{\Lambda}\text{Be}) < (2.0 \pm 0.4_{\text{stat}}^{+0.3}_{-0.1\text{syst}}) \cdot 10^{-5}/K_{\text{stop}}^-$ , which lowers by a factor  $\sim 3$  the previous KEK determination [8].

Recently, analyzing the complete available data sample, the FINUDA experiment has reported an experimental evidence for the existence of  ${}^6_{\Lambda}\text{H}$  [11, 12]. The increased statistics has been exploited to reduce the overwhelming background events in reaction (1) with  $K^-$  at rest by requiring a coincidence with  $\pi^-$  mesons from the two-body weak decay of the produced hypernucleus:



the same method has also been applied to the search of  ${}^9_{\Lambda}\text{He}$  produced on  ${}^9\text{Be}$  targets. In this paper a description of the coincidence technique is given and results on production rates are discussed.

## 2 Evidence for ${}^6_{\Lambda}\text{H}$ .

FINUDA was a hypernuclear physics experiment installed at one of the two interaction regions of the DAΦNE  $e^+e^-$  collider, the INFN-LNF Φ(1020)-factory. A description of the experimental apparatus can be found in [12]; we only recall the experimental features relevant to the present analysis. For  $\pi^+$  with momentum  $\sim 250$  MeV/c the resolution of the tracker, determined by means of the peak by monochromatic (236.5 MeV/c)  $\mu^+$  from  $K_{\mu 2}$  decay, is  $\sigma_p = (1.1 \pm 0.1)$  MeV/c [13], giving a resolution on the kinetic energy  $\sigma_T = 0.96$  MeV, and the precision on the absolute momentum calibration is better than 0.12 MeV/c for the  ${}^6\text{Li}$  targets, giving a systematic deviation on the kinetic energy  $\sigma_{T\text{syst}}(\pi^+) = 0.1$  MeV. For  $\pi^-$  with momentum  $\sim 130$  MeV/c the resolution and absolute calibration are evaluated from the peak of the monochromatic (132.8 MeV/c)  $\pi^-$  coming from the two-body weak decay of the  ${}^4_{\Lambda}\text{H}$  hyperfragment produced with a formation probability about  $10^{-3} - 10^{-2}$  per stopped  $K^-$  [14]: a resolution  $\sigma_p = (1.2 \pm 0.1)$  MeV/c, giving  $\sigma_T = 0.84$  MeV, and a precision of 0.2 MeV/c, giving a systematic deviation of the kinetic energy  $\sigma_{T\text{syst}}(\pi^-) = 0.14$  MeV, were found. Fig. 1 shows the FINUDA reconstructed momentum distributions of  $K_{\mu 2}$  decay  $\mu^+$ 's and 132.8 MeV/c  $\pi^-$ 's.

Since the stopping time of  ${}^6_{\Lambda}\text{H}$  in metallic Li is shorter than its lifetime (about 260 ps, the free  $\Lambda$  lifetime), both production (3) and decay (4) occur at rest; a simple algebra leads to the following

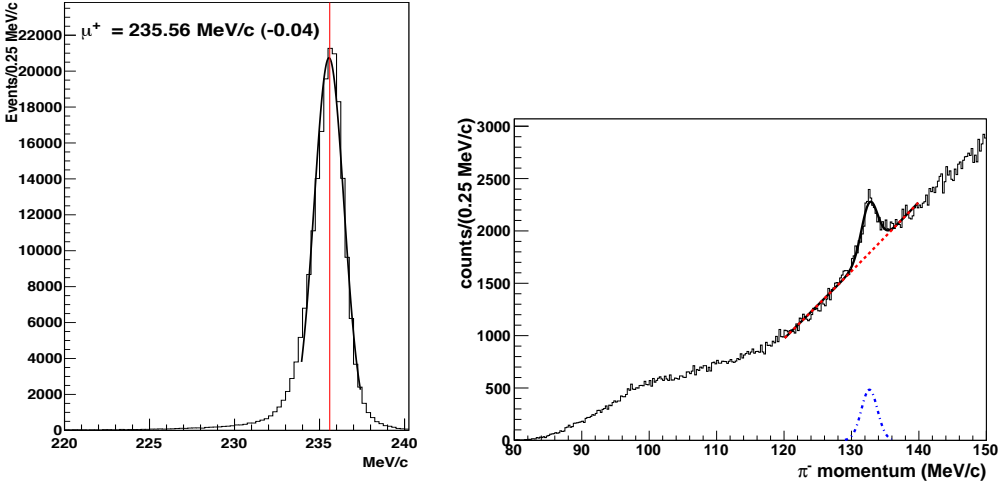


**Figure 1.** Left: performance on the momentum distribution of  $K_{\mu 2}$  decay  $\mu^+$ . From [13]. Right: distribution of low momentum  $\pi^-$  from the two  ${}^6\text{Li}$  targets; the peak corresponds to the  ${}^4_{\Lambda}\text{H} \rightarrow {}^5\text{He} + \pi^-$  decay at rest. From [12].

expression for  $T_{\text{sum}} \equiv T(\pi^+) + T(\pi^-)$ :

$$T_{\text{sum}} = M(K^-) + M(p) - M(n) - 2M(\pi) - B({}^6\text{Li}) + B({}^6\text{He}) - T({}^6\text{He}) - T({}^6_{\Lambda}\text{H}), \quad (5)$$

in which  $M$  stands for known masses,  $B$  for known nuclear binding energies, and  $T$  for kinetic energies. The value of  $T_{\text{sum}}$  varies merely by 50 keV upon varying  $B_{\Lambda}({}^6_{\Lambda}\text{H})$  by 1 MeV, therefore negligibly with respect to the experimental energy resolution for a  $\pi^{\pm}$  pair in coincidence,  $\sigma_T = 1.28$  MeV as obtained from both experimental and systematic uncertainties on  $\pi^+$  and  $\pi^-$  kinetic energies. Evaluating the r.h.s. of Eq. (5) by assuming  $B_{\Lambda}({}^6_{\Lambda}\text{H}) = 5$  MeV, from the average of 4.2 and 5.8 MeV predicted in Refs. [1, 5], one obtains  $T_{\text{sum}} = 203 \pm 1.3$  MeV for  ${}^6_{\Lambda}\text{H}$  candidate events.

In the analysis events in the interval  $T_{\text{sum}} = (203 \pm 1)$  MeV were considered, as a compromise between the contamination from background reactions discussed in more detail below, and the available statistics.

Fig. 2 (left) shows a 2-d plot in the  $(p_{\pi^-}, p_{\pi^+})$  plane for coincidence events selected in the band  $T_{\text{sum}} = 202 - 204$  MeV. The distribution drops above  $p_{\pi^+} \simeq 245$  MeV/c and below  $p_{\pi^-} \simeq 145$  MeV/c. This is close to the region where  ${}^6_{\Lambda}\text{H}$  events are expected. To search for particle-stable  ${}^6_{\Lambda}\text{H}$  events below its  $({}^4_{\Lambda}\text{H} + 2n)$  lowest threshold (see Fig.4 left for a scheme of particle emission thresholds), using the two-body kinematics of Eqs. (3) and (4), a further requirement of  $p_{\pi^+} > 251.9$  MeV/c and  $p_{\pi^-} < 135.6$  MeV/c is necessary. The ranges  $p_{\pi^+} = (250 - 255)$  MeV/c and  $p_{\pi^-} = (130 - 137)$  MeV/c were selected, covering a  ${}^6_{\Lambda}\text{H}$  mass range from the  $(\Lambda + {}^3\text{H} + 2n)$  threshold, about 2 MeV in the  ${}^6_{\Lambda}\text{H}$  continuum (see Fig. 4 left), down to a  ${}^6_{\Lambda}\text{H}$  bound somewhat stronger than predicted by Akaishi *et al.* [5]. This does not completely exclude possible contributions from the production and decay of  $({}^4_{\Lambda}\text{H} + 2n)$ : a complete discussion of the analysis technique can be found in [11, 12].

The outcome of the selection cuts on  $T_{\text{sum}}$  and on the  $p_{\pi^+}$  and  $p_{\pi^-}$  intervals is shown in details in Fig. 3, where a view of the 2-d plot in the  $(p_{\pi^-}, p_{\pi^+})$  plane for all coincidence events is reported, with a magnification of the signal region (see Fig. 3 of [12] for the original plot). The combined cuts on the  $p_{\pi^+}$  and  $p_{\pi^-}$  intervals (orange and blue horizontal and vertical lines) strongly reduce the background due to  $\Sigma^+$  production (at rest) and decay (in flight), as discussed in section 2.1; they also define different  $B_{\Lambda}$  ranges for  ${}^6_{\Lambda}\text{H}$ : the mean scanned  $B_{\Lambda}$  interval is 2.3-7.1 MeV. The cut  $T_{\text{sum}} =$

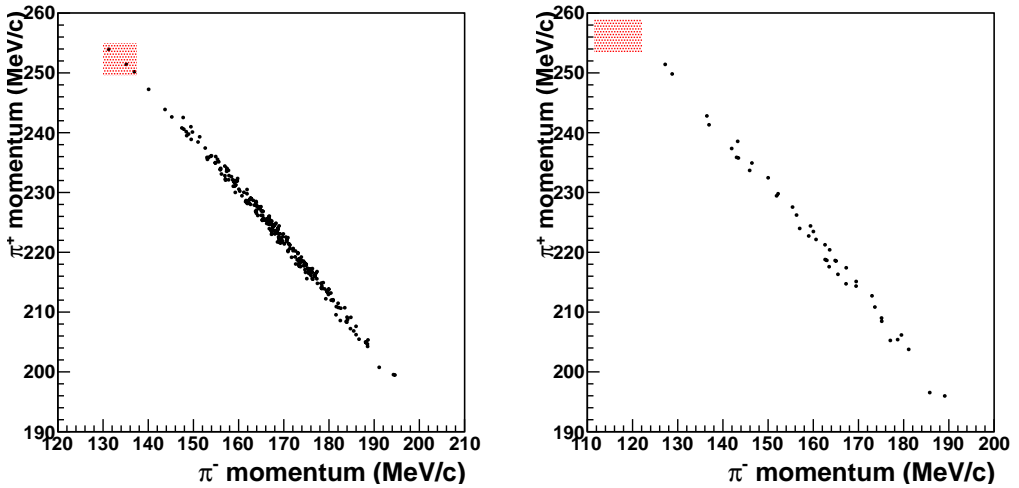


**Figure 2.** Left:  $\pi^+$  momentum vs  $\pi^-$  momentum for  ${}^6\text{Li}$  target events with  $T_{\text{sum}} = 202 - 204$  MeV. The red area consists of a subset of events with  $p_{\pi^+} = 250 - 255$  MeV/c and  $p_{\pi^-} = 130 - 137$  MeV/c. Right:  $\pi^+$  momentum vs  $\pi^-$  momentum for  ${}^9\text{Be}$  target events with  $T_{\text{sum}} = 194.5 - 197.5$  MeV. The red area indicates the expected position of events with  $p_{\pi^+} = 253.5 - 259$  MeV/c and  $p_{\pi^-} = 114.5 - 122$  MeV/c.

202-204 MeV (blue and magenta oblique lines) requires that, within the chosen 2 MeV tolerance, the mass of the produced system is equal to that of the decaying one, strongly reducing the possibility of detecting events where  ${}^6_{\Lambda}\text{H}$  is produced in an excited state above the ( ${}^4_{\Lambda}\text{H} + 2n$ ) lowest threshold, which then decays strongly to  ${}^4_{\Lambda}\text{H}$  with the subsequent emission of a  $\sim 133$  MeV/c  $\pi^-$ . It is evident from Fig. 3 that the  $T_{\text{sum}}$  cut is very effective in identifying the production and decay of a stable  ${}^6_{\Lambda}\text{H}$ , while by releasing this selection the production of excited hyper-hydrogen states not stable with respect to strong interaction would be possible, as for the green oblique lines which represents the  $T_{\text{sum}} = 200-206$  MeV cut.

Out of a total number of  $\sim 2.7 \cdot 10^7$   $K^-$  stopped in the  ${}^6\text{Li}$  targets, we found three events that satisfy the final requirements, as shown within the red area in Fig. 2 left. Different choices of  $T_{\text{sum}}$  interval widths (2 – 6 MeV) and position (center in 202 – 204 MeV), and of  $p_{\pi^\pm}$  interval widths (5 – 10 and 8 – 15 MeV/c respectively) with fixed limits at 250 and 137 MeV/c respectively to exclude the unbound region, do not affect the population of the selected region. For example, no new candidate events appear in the shaded area upon extending the cut  $T_{\text{sum}} = 202 - 204$  MeV to  $T_{\text{sum}} = 200 - 206$  MeV. A similar stability is not observed in the opposite corner of Fig. 2 left where, on top of the events already there, six additional events appear. Quantitatively, fitting the projected  $\pi^\pm$  distributions of Fig. 2 (left) by gaussians, an excess of three events in both  $p_{\pi^\pm}$  distributions is invariably found, corresponding to the shaded (red) area. The probability for the three events to belong to the fitted gaussian distribution is less than 0.5% in both cases. This rules out systematic errors associated with the present analysis selection.

The three  ${}^6_{\Lambda}\text{H}$  candidate events are listed in Table 1 together with nuclear mass values derived separately from production (3) and from decay (4); the errors reported are evaluated directly from the tracker resolution for  $\pi^+$  and  $\pi^-$  discussed before. These mass values yield a mean value  $M({}^6_{\Lambda}\text{H}) = (5801.4 \pm 1.1)$  MeV, jointly from production and decay where the error is given by the spread of the average mass values for the three events.

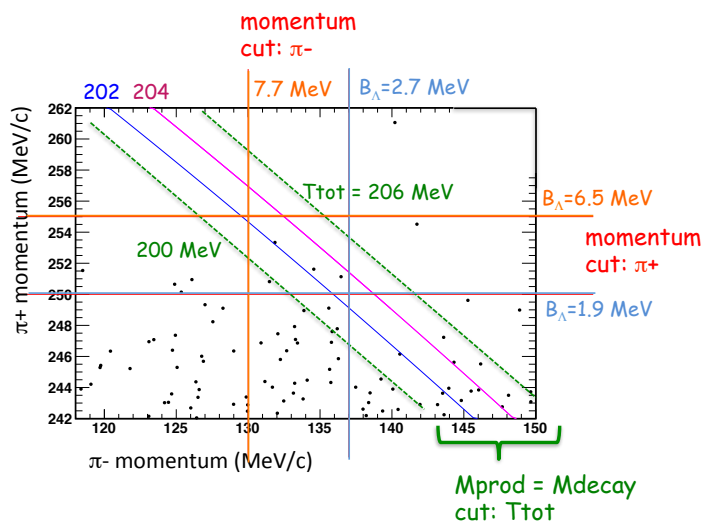


**Figure 3.** Expanded view of the  $(p_{\pi^-}, p_{\pi^+})$  plane for coincidence events, magnified in the  ${}^6_{\Lambda}\text{H}$  signal region. Horizontal and vertical lines represents the cuts on  $p_{\pi^+}$  and  $p_{\pi^-}$  applied in the analysis; oblique lines represents different cuts on  $T_{\text{sum}}$ . See text for more details.

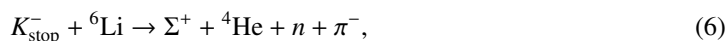
**Table 1.** Summed kinetic energy  $T_{\text{sum}} = T(\pi^+) + T(\pi^-)$ , pion momenta  $p_{\pi^\pm}$ , and mass values inferred for the three  ${}^6_{\Lambda}\text{H}$  candidate events from production (3) and decay (4). The mean mass value is  $M({}^6_{\Lambda}\text{H}) = (5801.4 \pm 1.1)$  MeV, see text.

$T_{\text{sum}}$ (MeV)	$p_{\pi^+}$ (MeV/c)	$p_{\pi^-}$ (MeV/c)	$M({}^6_{\Lambda}\text{H})_{\text{prod.}}$ (MeV)	$M({}^6_{\Lambda}\text{H})_{\text{decay}}$ (MeV)
$202.6 \pm 1.3$	$251.3 \pm 1.1$	$135.1 \pm 1.2$	$5802.33 \pm 0.96$	$5801.41 \pm 0.84$
$202.7 \pm 1.3$	$250.1 \pm 1.1$	$136.9 \pm 1.2$	$5803.45 \pm 0.96$	$5802.73 \pm 0.84$
$202.1 \pm 1.3$	$253.8 \pm 1.1$	$131.2 \pm 1.2$	$5799.97 \pm 0.96$	$5798.66 \pm 0.84$

Furthermore, we note from Table 1 that the mass values associated with production are systematically higher than those evaluated from the decay, by  $(0.98 \pm 0.74)$  MeV. These mass differences could be connected to the excitation spectrum of  ${}^6_{\Lambda}\text{H}$ .

## 2.1 Background estimate, production rate and discussion

A complete simulation of  $K_{\text{stop}}^-$  absorption reactions on single nucleons was performed, as well as on correlated few-nucleon clusters, that lead to the formation and decay of  $\Lambda$  and  $\Sigma$  hyperons. Full details can be found in [12], here it is sufficient to focus on one chain of reactions likely to produce  $\pi^\pm$  coincidences overlapping with those selected to satisfy  ${}^6_{\Lambda}\text{H}$  production (3) and decay (4):  $\Sigma^+$  production



where  $p_{\pi^-} \leq 190 \text{ MeV}/c$ , followed by  $\Sigma^+$  decay in flight

$$\Sigma^+ \rightarrow n + \pi^+ \quad [p_{\pi^+} \leq 282 \text{ MeV}/c]. \quad (7)$$

The  $\Sigma^+$  production was treated in the quasi-free approach, following the analysis of the FINUDA experiment observing  $\Sigma^\pm \pi^\mp$  pairs [15]; in the signal region a small contribution of  $(0.16 \pm 0.07)$  expected events was evaluated. The reaction chain of  ${}^4_\Lambda\text{H}$  hyperfragment production and two body decay, strongly reduced by the cut on  $T_{tot}$ , has been estimated to deliver a negligible background of  $(0.04 \pm 0.01)$  expected events. All other reaction chains that could produce  $\pi^\pm$  coincidences within the described selection ranges were ruled out by the selections applied. Turning to potential instrumental backgrounds, we note that these could result from fake tracks, filtered because of reconstruction errors. To this end we considered, with the same cuts, events coming from different nuclear targets used in the same runs ( ${}^7\text{Li}$ ,  ${}^9\text{Be}$ ,  ${}^{13}\text{C}$ ,  ${}^{16}\text{O}$ ). We found one event coming from  ${}^9\text{Be}$  and accordingly evaluate as  $0.27 \pm 0.27$  the expected fake events from  ${}^6\text{Li}$ , due to instrumental background.

A total background of  $(0.43 \pm 0.28)$  expected events was evaluated. Thus, using Poisson distribution, the three  ${}^6_\Lambda\text{H}$ -assigned events do not arise from background to a confidence level of 99%. The statistical significance of the result is  $S=3.9$ .

Given the above background estimates, plus efficiency, target purity and cut estimates, it is possible to evaluate the product  $R(\pi^+) \cdot \text{BR}(\pi^-)$ , where  $R(\pi^+)$  is the  ${}^6_\Lambda\text{H}$  production rate per  $K_{\text{stop}}^-$  in reaction (3) and  $\text{BR}(\pi^-)$  the branching ratio for the two-body  $\pi^-$  decay (4):

$$R(\pi^+) \cdot \text{BR}(\pi^-) = (2.9 \pm 2.0) \cdot 10^{-6} / K_{\text{stop}}^-. \quad (8)$$

Assuming  $\text{BR}(\pi^-) = 49\%$ , as for the analogous  ${}^4_\Lambda\text{H} \rightarrow {}^4\text{He} + \pi^-$  decay [14], we find  $R(\pi^+) = (5.9 \pm 4.0) \cdot 10^{-6} / K_{\text{stop}}^-$ , fully consistent with the previous FINUDA results [10]. This production rate  $R(\pi^+)$  is two to three orders of magnitude smaller than summed  $\Lambda$ -bound production rates  $R(\pi^-)$  of normal light  $\Lambda$  hypernuclei in the  $(K_{\text{stop}}^-, \pi^-)$  reaction [13].

Table 1 yields a mean value  $B_\Lambda({}^6_\Lambda\text{H}) = (4.0 \pm 1.1) \text{ MeV}$  with respect to  $({}^5\text{H} + \Lambda)$ , as shown in Fig. 4, in good agreement with the estimate 4.2 MeV [1] but considerably short of Akaishi's prediction  $B_\Lambda^{\text{th}}({}^6_\Lambda\text{H}) = 5.8 \text{ MeV}$  [5]. This indicates that coherent  $\Lambda N - \Sigma N$  mixing in the  $s$ -shell hypernucleus  ${}^4_\Lambda\text{H}$  [16] becomes rather ineffective for the excess  $p$  shell neutrons in  ${}^6_\Lambda\text{H}$ .

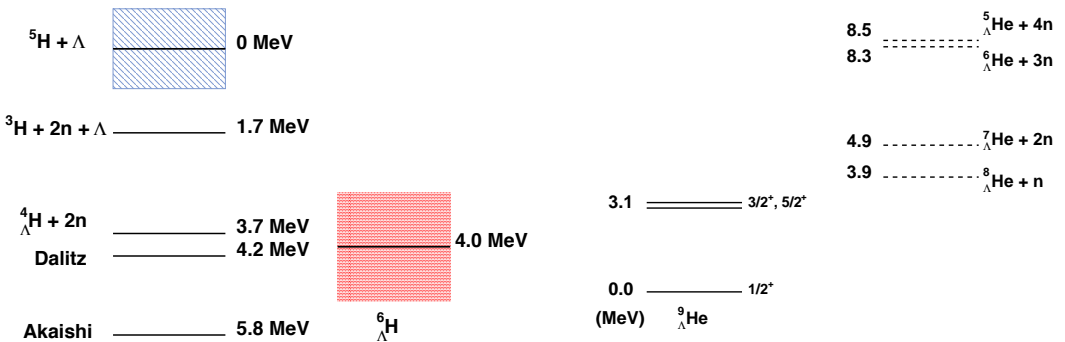


**Figure 4.** Left:  ${}^6_\Lambda\text{H}$  binding energy with respect to  $({}^5\text{H} + \Lambda)$  from three candidate events, as related to several particle emission thresholds and theoretical predictions. From [12]. Right:  ${}^9_\Lambda\text{He}$  neutron emission thresholds with respect to the g.s.. From [17]. The two schemes are not in scale.

The three events that give evidence for a particle-stable  ${}^6_{\Lambda}\text{H}$  can also give additional information on its excitation spectrum. It is expected to consist of a  $0^+$  g.s. and  $1^+$  excited state as in  ${}^4_{\Lambda}\text{H}$  (1.04 MeV), and a  $2^+$  excited state as for the  $p$ -shell dineutron system in  ${}^6\text{He}$  (1.80 MeV). In fact, it is  ${}^6_{\Lambda}\text{H}(1^+)$  that is likely to be produced in reaction (3) simply because Pauli spin is conserved in production at rest, and the Pauli spin of  ${}^6\text{Li}$  is  $S = 1$  to better than 98%. The weak decay (4), however, appears to occur from a lower state (reasonably  ${}^6_{\Lambda}\text{H}(0^+)$  g.s.): the (unseen)  $\gamma$  transition  $1^+ \rightarrow 0^+$  should be about three orders of magnitude faster than weak decay. Indeed, the production vs decay mass difference ( $0.98 \pm 0.74$ ) MeV extracted from the three  ${}^6_{\Lambda}\text{H}$  events listed in Table 1 is comparable to the underlying 1.04 MeV  $1^+$  excitation in  ${}^4_{\Lambda}\text{H}$ . In this case the  $B_{\Lambda}$  value for the g.s. would be larger  $B_{\Lambda}({}^6_{\Lambda}\text{H}_{\text{g.s.}}) = (4.5 \pm 1.2)$  MeV. This scenario requires further experimental as well as theoretical inquiries.

### 3 Search for ${}^9_{\Lambda}\text{He}$

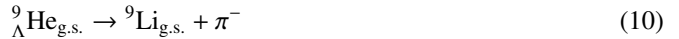
The neutron-rich hypernucleus  ${}^9_{\Lambda}\text{He}$  is one of the exotic  $\Lambda$ -hypernuclear species considered decades ago in [1] and by Majling [3] who estimated  $B_{\Lambda}({}^9_{\Lambda}\text{He}) = 8.5$  MeV. Fig. 4 on the right shows the  ${}^9_{\Lambda}\text{He}$  g.s. level, indicated with 0.0 MeV energy, together with neutron emission thresholds below the 8.5 MeV  $\Lambda$  emission threshold.

Since  ${}^9\text{Be}$  targets were used in the same data taking of FINUDA in which  ${}^6_{\Lambda}\text{H}$  was produced on  ${}^6\text{Li}$  targets, with a similar number of stopped  $K^-$ , the possibility was examined whether the method applied to the successful search for  ${}^6_{\Lambda}\text{H}$  could be extended to the case of  ${}^9_{\Lambda}\text{He}$ . Full details can be found in [17].

${}^9_{\Lambda}\text{He}$  could be produced in the two-body reaction:



Assuming  $B_{\Lambda}({}^9_{\Lambda}\text{He}) = 8.5$  MeV, it is straightforward to evaluate the momentum  $p_{\pi^+} = 257.5$  MeV/c for a  $\pi^+$  meson emitted in (9). Since  ${}^9\text{Li}$  g.s. is particle stable [18], admitting thus a two-body weak decay:



producing a  $\pi^-$  meson with  $p_{\pi^-} = 116.9$  MeV/c, the coincidence method could indeed be applied. Observing that, also in this case, formation (9) and decay reaction (10) occur at rest, since the stopping time of  ${}^9_{\Lambda}\text{He}$  in the material (Be) is shorter than its lifetime (about 260 ps, the free  $\Lambda$  lifetime), from momentum and energy conservation it is immediate to derive an equation analogous to (5):

$$T_{\text{sum}} = M(K^-) + M(p) - M(n) - 2M(\pi) - B({}^9\text{Be}) + B({}^9\text{Li}) - T({}^9\text{Li}) - T({}^9_{\Lambda}\text{He}) \quad (11)$$

in which, again,  $M$  stands for known masses,  $B$  for known nuclear binding energies, and  $T$  for kinetic energies. The value of  $T_{\text{sum}}$  varies by 10 keV upon varying  $B_{\Lambda}({}^6_{\Lambda}\text{H})$  by 1 MeV, negligible with respect to the experimental energy resolution discussed before. By considering a value of  $B_{\Lambda}({}^9_{\Lambda}\text{He}) = 8.5$  MeV [3],  $T_{\text{sum}} = (195.8 \pm 1.3)$  MeV.

In this case, for the ( $\pi^+$ ,  $\pi^-$ ) coincidence only events for which  $T_{\text{sum}}$  assumed values in the range (194.5 – 197.5) MeV were considered. The two-dimensional plot of these selected events is shown in Fig. 2 right. Events associated with the formation of  ${}^9_{\Lambda}\text{He}$  with values of  $B_{\Lambda}({}^9_{\Lambda}\text{He})$  varying between 5 and 10 MeV should fall in the red area in the figure, corresponding to  $p_{\pi^+} = (253.5 - 259)$  MeV/c and  $p_{\pi^-} = (114.5 - 122)$  MeV/c. From Fig. 4 it is possible to see that a binding energy of 5 MeV is about 0.5 MeV below the lowest neutron emission threshold expected for  ${}^9_{\Lambda}\text{He}$ . There are clearly no events satisfying the conditions required by the formation and decay of  ${}^9_{\Lambda}\text{He}$  with  $B_{\Lambda}({}^9_{\Lambda}\text{He}) \geq 5$  MeV.

It was thus possible to derive an upper limit for  ${}^9_{\Lambda}\text{He}$  production rate  $R \cdot \text{BR}(\pi^-)$ , where  $R$  is  ${}^9_{\Lambda}\text{He}$  production rate per stopped  $K^-$  in reaction (9) and  $\text{BR}(\pi^-)$  is the branching ratio (BR) for  ${}^9_{\Lambda}\text{He}$  two-body weak decay (10). Considering a 90% confidence level (C.L.), plus efficiency and cut estimates it was obtained:

$$R \cdot \text{BR}(\pi^-) \leq \frac{N}{\epsilon(\pi^+) \epsilon(\pi^-) K_{\text{stop}}^- ({}^9\text{Be})} < (2.3 \pm 1.9) \cdot 10^{-6} / K_{\text{stop}}^- \rightarrow 4.2 \cdot 10^{-6} / K_{\text{stop}}^- \quad (12)$$

If for  $\text{BR}(\pi^-)$  the value of 0.261 is assumed, following the calculations of [19], an upper limit is obtained for  $R$  of  $(2.3 + 1.9)/0.261 \cdot 10^{-6} / K_{\text{stop}}^- = 1.6 \cdot 10^{-5} / K_{\text{stop}}^-$  (at 90% C.L.) [17], improving by over an order of magnitude the previous upper limit set in KEK experiment [8].

## 4 Conclusions

FINUDA has presented the first evidence for heavy hyper-hydrogen  ${}^6_{\Lambda}\text{H}$ , based on detecting three events shown to be clean of instrumental and/or physical backgrounds. The derived binding energy of  ${}^6_{\Lambda}\text{H}$  limits the strength of the coherent  $\Lambda N - \Sigma N$  mixing effect predicted in neutron-rich strange matter [5], together with the conjectured  $0^+ - 1^+$  doublet splitting. FINUDA has also derived an upper limit for the production of the  ${}^9_{\Lambda}\text{He}$  hypernucleus, based on the same method of detecting a  $\pi^-$  weak decay in coincidence. A search of  ${}^6_{\Lambda}\text{H}$  and  ${}^9_{\Lambda}\text{He}$  in the  $(\pi^-, K^+)$  reaction at 1.2 GeV/c on  ${}^6\text{Li}$  and  ${}^9\text{Be}$ , respectively, is scheduled at J-PARC.

## References

- [1] R.H. Dalitz and R. Levi Setti, *Nuovo Cimento* **30** (1963) 489.
- [2] M. Jurić et al., *Nucl. Phys.* **B 52** (1973) 1.
- [3] L. Majling, *Nucl. Phys.* **A 585** (1995) 211c.
- [4] D.R. Tilley et al., *Nucl. Phys.* **A 745** (2004) 155.
- [5] Y. Akaishi and T. Yamazaki, in *Frascati Physics Series XVI* (1999) 59; S. Shinmura, K.S. Myint, T. Harada, and Y. Akaishi, *J. Phys. G* **28** (2002) L1; for a recent review, see Y. Akaishi and K.S. Myint, *AIP Conf. Proc.* **1011** (2008) 277, Y. Akaishi, *Prog. Theor. Phys. Suppl.* **186** (2010) 378, and references therein.
- [6] J. Schaffner-Bielich, *Nucl. Phys.* **A 804** (2008) 309, *Nucl. Phys.* **A 835** (2010) 279.
- [7] R.E. Chrien, C.B. Dover, A. Gal, *Czech. J. Phys.* **42** (1992) 1089.
- [8] K. Kubota et al., *Nucl. Phys.* **A 602** (1996) 327.
- [9] P.K. Saha et al., *Phys. Rev. Lett.* **94** (2005) 052502.
- [10] M. Agnello et al., *Phys. Lett.* **B 640** (2006) 145.
- [11] M. Agnello et al., *Phys. Rev. Lett.* **108** (2012) 042501.
- [12] M. Agnello et al., *Nucl. Phys.* **A 881** (2012) 269.
- [13] M. Agnello et al., *Phys. Lett.* **B 698** (2011) 219.
- [14] H. Tamura et al., *Phys. Rev.* **C 40** (1989) R479.
- [15] M. Agnello et al., *Phys. Lett.* **B 704** (2011) 474.
- [16] Y. Akaishi, T. Harada, S. Shinmura, and K.S. Myint, *Phys. Rev. Lett.* **84** (2000) 3539.
- [17] M. Agnello et al., *Phys. Rev.* **C86** (2012) 057301.
- [18] see <http://www.nndc.bnl.gov/> for nuclear data compilation.
- [19] A. Gal, *Nucl. Phys.* **A828** (2009) 72.